Drone-to-Drone Propagation Characteristics in Urban Safety-Critical Scenarios

Dennis Becker*, Uwe-Carsten Fiebig*, Lukas Marcel Schalk*,
*Institute of Communications and Navigation
German Aerospace Center (DLR)
Oberpfaffenhofen-Wessling, Germany
dennis.becker@dlr.de

***Abstract*—For the future Urban Air Mobility we expect a highly frequented urban air space with many autonomously flying unmanned aircraft, often called drones. In order to mitigate the risk of mid-air collisions in high dense drone scenarios, a robust and reliable information exchange between all airspace users based on direct Drone-to-Drone communication will be an essential part. But due to the high mobility of drones and the strong multipath propagation in urban environments, a communication system must be specifically designed for being able to cope with those challenging conditions. Therefore, we performed a channel sounding measurement campaign in order to investigate the specific Drone-to-Drone propagation characteristics in urban environments and identified stronger multipath components sources for different scenarios in previous work. In this work, we first analyze and present the propagation characteristics for a highly safety-critical scenario, in which the drones are on collision course with changing propagation conditions. Secondly, we use the findings to simulate and discuss the influence on a transmission system. Furthermore, we show when certain propagation effects can be beneficial for the communication in terms of collision avoidance.**

***Index Terms*—unmanned aerial vehicle, air-to-air, propagation, drone-to-drone communication, safety-critical scenarios**

I. Introduction

For a safe and efficient integration of unmanned aircraft into urban airspace, the traffic management will have to be carried out differently than today as high expected traffic densities and very short reaction times will make the remote control unmanned aerial vehicles unfeasible. A redundant higher-level safety net taking care of the coordination and monitoring of the traffic is common in today's civil aviation [1]–[3] and maritime domain [4] and already planned for future railway traffic [5] and autonomous driving [6], [7]. But for UAVs it is still missing and we see the need for an additional robust communications concept that enables a reliable information exchange between UAVs. In order to avoid mid-air collisions between all flying urban airspace users in dense urban areas, we see direct Drone-to-Drone (D2D) communications as a promising approach for reliably sharing important information with very low latency. To the best of our knowledge, there is currently no commercial communication system available that addresses the future requirements for the safe and efficient information exchange between drones while considering the specific and challenging signal propagation characteristics in urban environments. The transmitted electromagnetic signals are reflected, scattered, and diffracted by a variety of objects like buildings and trees, leading to a rich multipath environment. At the receiver, fading due to numerous, overlapping multipath signals may occur and might yield to communication outages. In addition, we expect strong non-line-of-sight (NLOS) conditions due to shadowing by surrounding buildings with the consequence that drones cannot receive any signals or only weak reflected and diffracted signal components. From a physical layer point-of-view a transmission system must deal with the specific delay and Doppler frequency spreads, which are detrimental because it leads to fading in frequency and time domain that decreases the received power at the receiver depending on constructive or destructive interference. The transmitted symbol duration must be long enough to avoid inter symbol interference, but this can limit the achievable data rate or increase channel equalizer complexity. Therefore, we are aiming for a dedicated Drone-to-Drone communication and surveillance system that performs reliably in safety-critical scenarios, while experiencing challenging communication channel conditions. As a first step towards this, we have conducted a wideband channel measurement campaign in order to accurately measure the D2D propagation characteristics in an urban environment [8], [9]. Our first findings have shown that the urban D2D communication channel exhibits rich multipath and shadowing characteristics.

In this work, we analyze the measured Drone-to-Drone propagation characteristics for a safety-critical scenario in which drones are on collision courses while not being in line-of-sight to each other and experiencing poor channel characteristics. We compare the measured propagation effects with deterministic approaches that model shadowing and diffraction on all signal paths between transmitter and receiver. Eventually, we present the received signal power for a selected safety-critical scenario and identify situations which may lead to collisions of drones due to shadowing or destructive interference of signals. Furthermore, we identify situations in which multipath propagation and diffraction can be beneficial for the information exchange between drones, because it can increase the radio range due to the constructive interference and signal reception in conditions when LOS signal path is shadowed.

TABLE I
CHANNEL SOUNDING PARAMETERS

Parameter	Symbol	Value
Center frequency	f_c	5.2 GHz
Bandwidth	B	100 MHz
Tx Power	P_{tx}	30 dBm
Signal duration	T_p	12.8 μs
Signal period	T_g	1.024 ms
Time resolution	Δt	10 ns
Max resolvable Doppler freq.	$f_{d_{\text{max}}}$	488 Hz
ADC resolution	res_{adc}	8 bit
Dynamic range	α_{agc}	52 dB
Antenna Tx		omni-dir. V-polarized 0 dBi
Antenna Rx		omni-dir. V-polarized 0 dBi

II. MEASURED SAFETY-CRITICAL SCENARIO IN AN URBAN ENVIRONMENT

We performed a Drone-to-Drone wideband channel sounding measurement campaign at C-Band with two flying small hexacopters in an urban environment at our campus site in Oberpfaffenhofen, Germany. The measurement setup and used equipment was presented in more details in [8], but we summarize the important information as a foundation of this work in the following.

A. Measurement Parameters

Table I summarizes the most important parameters of our measurement system. We performed measurements in the C-Band at 5.2 GHz with 100 MHz bandwidth and a transmission power of 30 dBm. With the given setup we are able to resolve multipath components (MPCs) with propagation delays of up to 12.8 μs in steps of 10 ns, resulting in a spatial resolution of 3 m and a resolvable distance up to 1920 m for which the dynamic range of 52 dB is sufficient. Given a snapshot rate of 1.024 ms, the maximum resolvable Doppler frequency is 488 Hz, which is sufficient as the drones moved with speeds up to 1 m/s. The omni-directional and vertical polarized radiating antennas with gains of 0 dBi were mounted below the drones.

B. Safety-Critical Scenario

In this work we choose following flight scenario from our measurements, shown in Fig. 1. Two drones are flying at around 10 m height in an urban canyon below the rooftops of the surrounding buildings while being on collision course and experiencing different signal propagation conditions. "Drone TX" is transmitting the channel sounding signal, while "Drone RX" is receiving it. The 3D geometries of the surrounding buildings are plotted on top of a 2D satellite image. Fig. 2 shows the measured channel impulse response for 54 seconds of flight. We present the absolute received power at the receiver antenna. Several multipath components are visible and the one with lowest delay is the line-of-sight (LOS) component. The LOS component is not visible for the whole flight as the direct signal path is obstructed by a building first. The LOS component becomes visible at the end of the flight when the drones are flying towards each other around the buildings corner. When relying on communications for cooperative Detect-and-Avoid, but the transmission system suffers from outages due to challenging communication channel conditions, this scenario is highly safety-critical as the drones do not see each other until the collision occurs.

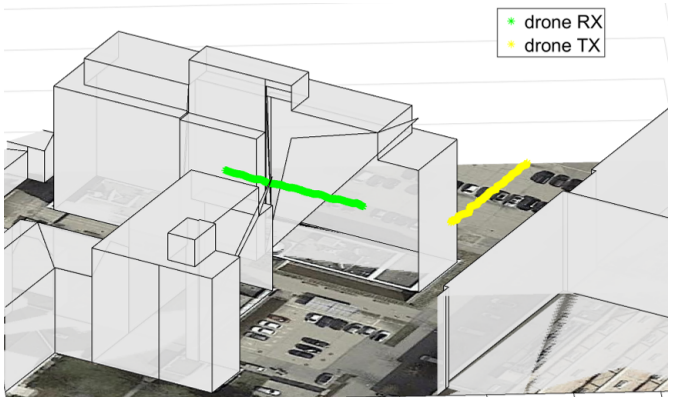

Fig. 1. Safety-critical Scenario in which the drones are on collision course when flying around a buildings corner in an urban environment.

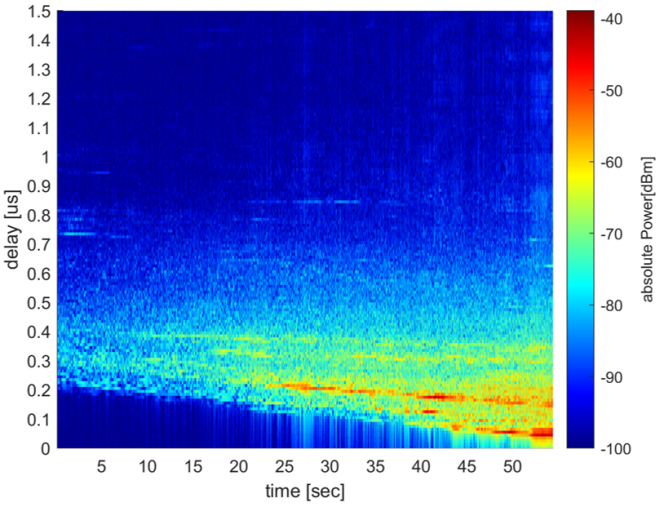

Fig. 2. Measured channel impulse response for the shown scenario.

III. METHOD

In this section we describe first, how we analyze the measured propagation characteristics for the given safety-critical scenario and second, how we investigate the influence of the findings on a transmission system.

A. Analyzing the Propagation Characteristics

In order to analyze the measured propagation characteristics, we first identify all the different signal components and follow our approach already presented and applied in [10], [11]. In the first step, we track all the multipath components with a tracking algorithm. After the tracking step, we are able to separate the components and analyze their power patterns as well as identify their origins. For the identification, we estimate the positions of the scatterer sources by utilizing the delay and Doppler frequency information directly from the

measurements of each signal component and analyze possible intersections with real world objects on two-dimensional satellite images and known three-dimensional geometries of the surrounding buildings. The existence of a LOS component can be easily identified if the position estimates of the component with lowest delays are located close to the direct signal path between the drones. Furthermore, we calculate the estimated freespace path loss (FSPL) for the LOS component with

$$A_{\text{FSPL,LOS}}=20\cdot\log 10\left[\frac{4\pi}{\lambda}dist_{\text{LOS}}\right] \tag{1}$$

given the direct distance $dist_{\text{LOS}}$ between the drones and the FSPL for the MPCs with

$$A_{\text{FSPL,MPC}}=20\cdot\log 10\left[\frac{4\pi}{\lambda}\left(dist_1+\Gamma dist_2\right)\right] \tag{2}$$

given the distances $dist_1 + dist_2$ between the drones and the localized scatterer source positions. The reflection loss Γ stands for the scatterer specific losses that are dependent on different parameters like the material, roughness and relative object size to the wavelength that influence the radiation behavior. Beside the FSPL, we also consider diffraction effects by the single knife-edge diffraction loss model presented in [12] and calculate the attenuation with

$$A_{\text{KE}}=20\cdot\log 10\Big[0.5\sqrt{[1-R(v)-I(v)]^2+[R(v)-I(v)]^2}\Big] \tag{3}$$

$$v=\sqrt{\frac{2dist_{\text{direct}}}{\lambda}\alpha_1\alpha_2} \tag{4}$$

$$Fres(v)=\frac{1+j}{2}\int_v^{\inf}\exp[\frac{-j\pi t^2}{2}]dt \tag{5}$$

$$R(v)=\Re(Fres(v)) \tag{6}$$

$$I(v)=\Im(Fres(v)) \tag{7}$$

given the direct distance $dist_{\text{direct}}$ between the transmitting and receiving position and the angles α_1 and α_2 between the direct path and the pathes between the transmitting and receiving antenna positions and the edge of the building. Fig. 3 illustrates the geometry for the two cases when the direct signal path is obstructed by a buildings edge and not. We present the direct signal path as being the LOS component, but it can be also a path received from a scatterer position instead of the transmitting antenna. The power at the receiving antenna is then calculated for FSPL with

$$L_{\text{RX,dBm}}=L_{\text{TX,dBm}}-A_{\text{FSPL,dB}} \tag{8}$$

and for single knife-edge diffraction loss with

$$L_{\text{RX,dBm}}=L_{\text{TX,dBm}}-A_{\text{FSPL,dB}}-A_{\text{KE,dB}} \tag{9}$$

Finally, we analyze the stochastic channel parameters and calculate the mean delay and Doppler frequency for the given

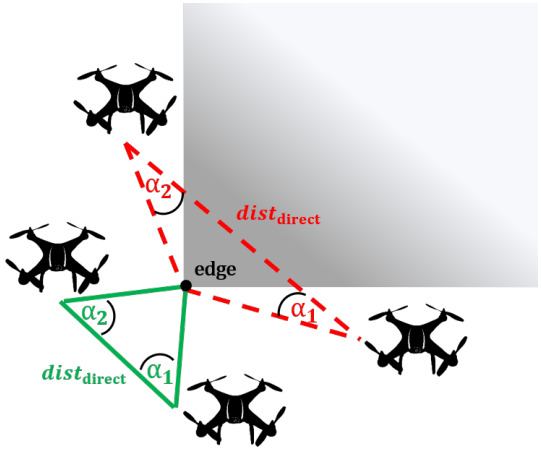

Fig. 3. Geometry of the single knife edge model for the two cases when the direct signal path is obstructed by a buildings edge and not.

scenario from the Power Delay Profile (PDP) and the Doppler Power Profile (DPP) with

$$m_\tau=\frac{\sum_{\tau=0}^{N_\tau}\tau P_{\text{PDP}}(\tau)}{\sum_{\tau=0}^{N_\tau}P_{\text{PDP}}(\tau)} \tag{10}$$

$$m_\nu=\frac{\sum_{\nu=0}^{N_\nu}\nu P_{\text{DPP}}(\nu)}{\sum_{\nu=0}^{N_\nu}P_{\text{DPP}}(\nu)} \tag{11}$$

and the delay and Doppler frequency spreads with

$$\sigma_\tau^2=\frac{\sum_{\tau=0}^{N_\tau}(m_\tau-\tau)^2P_{\text{PDP}}(\tau)}{\sum_{\tau=0}^{N_\tau}P_{\text{PDP}}(\tau)} \tag{12}$$

$$\sigma_\nu^2=\frac{\sum_{\nu=0}^{N_\nu}(m_\nu-\nu)^2P_{\text{DPP}}(\nu)}{\sum_{\nu=0}^{N_\nu}P_{\text{DPP}}(\nu)} \tag{13}$$

The coherence bandwidth and coherence time is then be estimated by lower bounds with

$$Bc\geq\frac{1}{2\pi\sigma_\tau} \tag{14}$$

$$Tc\geq\frac{1}{2\pi\sigma_\nu} \tag{15}$$

B. Investigating the Influence on a Transmission System

In order to discuss the theoretical influence on a transmission system, we calculate the received power by superimposing the measured powers P_{MPC_i} from all tracked N components with

$$L_{\text{RX}}=20\cdot\log 10\left[\sum_i^N P_{\text{MPC}_i}\exp(-j\Delta\Phi_{\text{MPC}_i})\right] \tag{16}$$

$$\Delta\Phi_{\text{MPC}_i}=\frac{2\pi C_0}{\lambda}\Delta t_{\text{MPC}_i} \tag{17}$$

given the measured delays Δt_{MPC_i} for the signal components. We then present the results with the theoretical power that would have been received when only considering the LOS component without multipath propagation and also without knife-edge diffraction loss and discuss when the propagation characteristics are beneficial or detrimental for a transmission system.

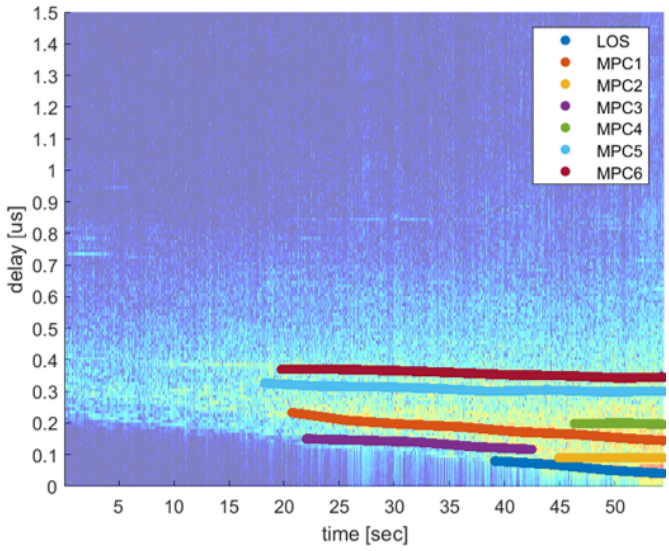

Fig. 4. Tracked components from channel impulse response.

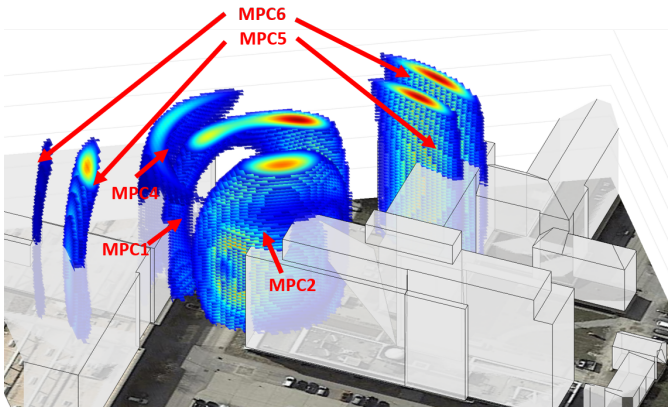

Fig. 5. Estimated scatterer positions for all tracked MPCs in 3d layout.

IV. D2D Propagation Characteristics

From the measured channel impulse presented in Fig. 2 we tracked in total seven significant signal components, consisting of a LOS component plus six MPCs. Fig. 4 shows all the tracked signal components. In the first twenty seconds of flight some signal power above noise floor are received, but no dominant signal component can be distinguished clearly. All the signal components have a certain lifetime and it can be seen from the LOS component that the drones do not see each other for most of the time as the direct path is obstructed the building in between them. Fig. 5 and Fig. 6 show the estimated scatterer positions as colored probability density functions in the space domain in a 2d and 3d layout from different viewing angles. Highly probable position estimates are colored in red. We identified the components by analyzing the intersections with known real world objects. Table II provides an overview of the identified scatterer sources. The estimated source position of MPC1 clearly

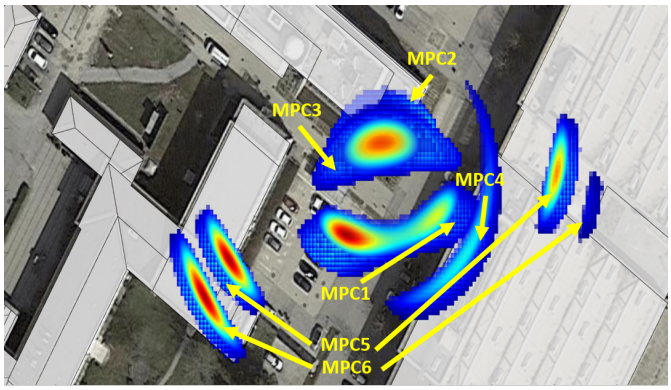

Fig. 6. Estimated scatterer positions for all tracked MPCs in 2d layout.

TABLE II
Identified Multipath Components

Name	Source Object	Type
LOS	direct path	line-of-sight component
MPC1	metallic surface of building	reflection
MPC2	object on rooftop	point scatterer
MPC3	bike station	point scatterer
MPC4	object on rooftop	point scatterer
MPC5	chimney/steelbeam on rooftop	point scatterer
MPC6	metallic ladder/stealbeam on rooftop	point scatterer

intersects with the surface of a building and by more detailed inspection, we see that it behaves more like a reflection that moves within a certain area on the surface. There is also an ambiguous position estimate around the parking lot in between the buildings, but now object was present at this area during measurements. Possible positions for MPC2 are present close to the building in between the drones and only objects on the rooftop right at the corner of this building can be a possible scatterer source. For MPC3 most likely a bike station with metallic roof in front of the building is the source as it intersects with the position estimates and is visible for both drones in the time period for this signal component. MPC4 is caused very likely by metallic objects on the rooftop of the building, which are close to the roof edge. For MPC5 and MPC6 the results are not clear as all the ambiguous position estimates intersect with real world objects. For each MPC two different objects would lead the same delay and Doppler frequencies when active as scatterer.

In Fig. 7 we show the received power when analyzing only the LOS component. Beside the measured power, also the estimated received powers for the freespace pathloss (FSPL) and the knife-edge diffraction model are presented. In order to analyze the LOS component for the whole flight, we first calculated the theoretical LOS signal delay without obstructions and read out the power values at the calculated delays. For the calculations of the knife-edge diffraction loss, we considered the uncertainties of the drone positions and the position of the buildings edge by changing the horizontal position of the edge within a circle of 1 m diameter and presenting the extreme

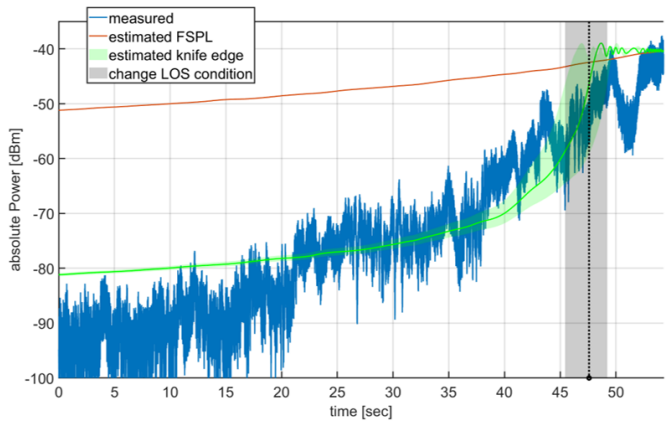

Fig. 7. Comparison of measured power for LOS component with freespace path loss and knife-edge diffraction loss for whole flight with changing propagation conditions.

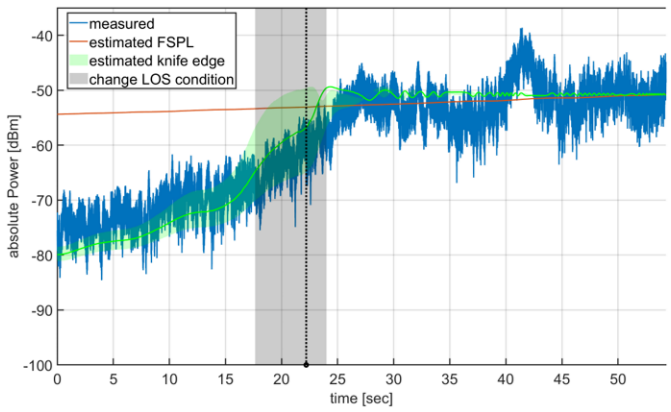

Fig. 8. Comparison of measured power for MPC1 component with freespace path loss and knife-edge diffraction loss for whole flight with changing propagation conditions.

values for the received power and the point in time when the drones start to see each other around the corner very likely. It can be seen, that the estimated power with FSPL only matches the measured power at the end of the flight, when the drones are in line-of-sight to each other. Before this change of LOS condition, the measured power matches the estimated power with knife-edge diffraction loss on top of FSPL. This result proofs the existence of the diffraction effect, that is sufficiently estimated by the single knife-edge model. The power of the LOS component does not suddenly drop to noise floor when starting to be obstructed by obstacles. Beside the general trend of the signal power, there are also some additional fluctuations of the signal power. Especially, when being in LOS to each other there is a significant drop in power. Reasons can be destructive interference with another multipath component that can not be resolved within the 10 ns time-grid or air frame shadowing by the drones themselves in a certain angle. Another reason can be the influence by the antenna pattern, which is not omni-directional in the elevation plane. Not only a changing viewing angle might change the antenna gain, also the drones might change their pitch angles as the drones start to slow down at this time in order to stop and fly back. In Fig. 8 we show the results when analyzing the signal component MPC1. Again the single knife-edge diffraction model matches the measurements well. The measurements reveal that the received signal power is relatively high when comparing to the estimated FSPL results and setting the reflection factor $\Gamma = 1$. The metallic surface is a relatively good reflector. For the given scenario we calculated the stochastic channel parameters given in table III.

V. Discussion of Influence on Transmission System

A reliable transmission system must be able to cope with signal distortions. In order to achieve nearly frequency-flat and time-flat channel conditions, for a single carrier system and depending on the complexity of the channel equalizer, the data

TABLE III
Stochastic Channel Parameters

Parameter	Symbol	Value
mean delay	m_τ	180 ns
rms delay spread	σ_τ	310 ns
mean Doppler	m_ν	11 Hz
rms Doppler spread	σ_ν	36 Hz
coherence bandwidth	B_c	0.51 MHz
coherence time	T_c	45 ms

rates should be kept lower than the coherence bandwidth and symbol duration must be longer than the delay spread while the maximum velocity should be kept low for experiencing higher coherence times. Otherwise significant drops in the signal power are experienced during reception leading to datalink outages. But when being able to cope with the experienced delay spreads or tolerating decreased link stability, multipath propagation can be beneficial as signals can be received in nonLOS conditions. This can help to increase the radio range and allow drones to communicate much earlier in safety-critical scenarios. In Fig. 9 we compare the received signal power for only the LOS component with the superimposed power from all signal components. For the superimposed signal power additional fading and significant power drops can be seen resulting from constructive and destructive self-interference. But in nonLOS conditions the signal power is higher on average and even almost reaches the estimated FSPL for longer distances. In order to get a feeling for the different radio ranges and link stability, we plotted the results on satellite maps by indicating in red when the signal power is above the threshold of -60 dBm and in blue when below the threshold. Fig. 10 shows the theoretical link availability for the case when only receiving the LOS signal component and Fig. 11 for the case when receiving all signal components.

VI. Conclusion

In this work, we presented the propagation characteristics and stochastic channel parameters for a measured safety-critical scenario with two drones on a collision course in

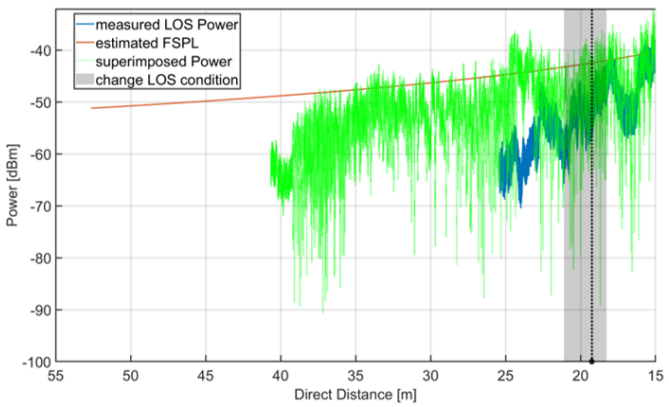

Fig. 9. Comparison of estimated freepace path loss with measured power for the tracked LOS component and the theoretical received power calculated by superimposing all tracked multipath component powers.

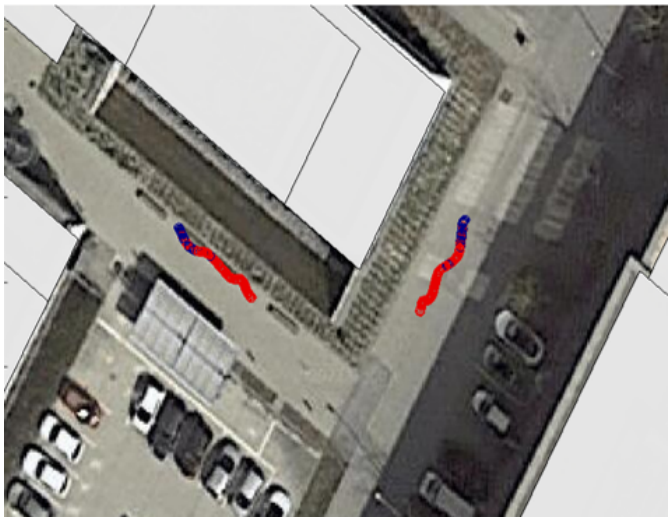

Fig. 10. Drone positions with indicated signal reception over threshold in red and below threshold in blue for a theoretical scenario, if only the LOS component would be received without multipath propagation.

an urban environment. We showed that multipath propagation with strong MPCs can be expected in such urban environments. We showed that signal paths are not only shadowed by buildings but also diffracted around corners and the diffraction loss matches the results from single knife-edge model. Furthermore, we discussed the possible influence on a transmission system with respect to the physical layer design and showed that utilizing multipath propagation can be beneficial in order to increase the radio range but can decrease link stability.The findings will help to develop a D2D channel model that considers the specific propagation characteristics in urban safety-critical scenarios and help for the physical layer design of an dedicated Drone-to-Drone communication and surveillance system with focus on cooperative collision avoidance.

Fig. 11. Drone positions with indicated signal reception over threshold in red and below threshold in blue for a theoretical scenario, if the receiver is receiving the superimposed signal with multipath propagation.

REFERENCES

[1] RTCA, DO-260B - Minimum Operational Performance Standards for 1090 MHz Extended Squitter Automatic Dependent Surveillance - Broadcast (ADS-B) and Traffic Information Services - Broadcast (TIS-B), 2009, Washington, DC, USA

[2] DO-282B with Corrigendum 1 - Minimum Operational Performance Standards for Universal Access Transceiver (UAT) Automatic Dependent Surveillance – Broadcast, 2011, Washing-ton, DC, USA

[3] FLARM, Technology, https://flarm.com/technology/

[4] ITU, Technical characteristics for an automatic identification system using time-division multiple access in the VHF maritime mobile band, Recommendation ITU-R M.1371-4, Apr. 2010

[5] T. Strang, “A Railway Collision Avoidance System exploiting Ad-hoc Inter-Vehicle Communications and GALILEO,” 13th World Congress and Exhibition on Intelligent Transportation Systems and Services (ITS 2006), p. 8, Oct. 2006.

[6] IEEE Standard for Information Technology–Local and Metropolitan Area Networks–Specific Requirements—Part 11: Wireless LAN Medium Access Control (MAC) and Physical Layer (PHY) Specifications Amendment 6: Wireless Access in Vehicular Environments,IEEE Standard 802.11p-2010, Jul. 2010.

[7] G. Naik, B. Choudhury, and J.-M. Park, “IEEE 802.11bd & 5G NR V2X: Evolution of Radio Access Technologies for V2X Communications,” IEEE Access, vol. 7, pp. 70169–70184, 2019, doi: 10.1109/ACCESS.2019.2919489.

[8] D. Becker and L. Schalk, ”Enabling Air-to-Air Wideband Channel Measurements between Small Unmanned Aerial Vehicles with Optical Fibers,” 2019 IEEE/AIAA 38th Digital Avionics Systems Conference (DASC), San Diego, CA, USA, 2019, pp. 1-7

[9] D. Becker, U. Fiebig and L. Schalk, ”Wideband Channel Measurements and First Findings for Low Altitude Drone-to-Drone Links in an Urban Scenario,” 2020 14th European Conference on Antennas and Propagation (EuCAP), Copenhagen, Denmark, 2020, pp. 1-5

[10] D. Becker, U.-C. Fiebig, and L. M. Schalk, “Approach for Localizing Scatterers in Urban Drone-to-Drone Propagation Environments,” in 2021 15th European Conference on Antennas and Propagation (EuCAP), Dusseldorf, Germany, Mar. 2021, pp. 1–5.

[11] D. Becker and U.-C. Fiebig, “Measurement Based Identification of MPCs in an Urban Drone-To-Drone Propagation Scenario,” presented at the 2022 16th European Conference on Antennas and Propagation (EuCAP), Madrid, 2022.

[12] ITU, “RECOMMENDATION ITU-R P.526-15 - Propagation by diffraction,” p. 45, 2019.